



## Post-spinning modification of electrospun nanofiber nanocomposite from *Bombyx mori* silk and carbon nanotubes

Milind Gandhi<sup>a</sup>, Heejae Yang<sup>a</sup>, Lauren Shor<sup>b</sup>, Frank Ko<sup>c,\*</sup>

<sup>a</sup>School of Biomedical Engineering, Sciences and Health System, Drexel University, Philadelphia, PA 19104, USA

<sup>b</sup>Department of Mechanical Engineering and Mechanics, Drexel University, Philadelphia, PA 19104, USA

<sup>c</sup>Canada Research Chair Professor (Tier I) of Advanced Fibrous Materials and Director of Advanced Materials and Process Engineering, University of British Columbia, 2355 East Mall, Vancouver, BC V6T 1Z4, Canada

### ARTICLE INFO

#### Article history:

Received 20 October 2008

Received in revised form

13 February 2009

Accepted 15 February 2009

Available online 25 February 2009

#### Keywords:

Silk nanofibers

Tissue engineering

Post-spinning

### ABSTRACT

Electrospinning is an effective procedure for fabricating submicron to nanoscale fibers from synthetic polymer as well as natural proteins. We successfully electrospun regenerated silk protein from cocoons of *Bombyx mori* to produce random as well as aligned fibers with diameter less than 100 nm. The fibers were characterized using field emission scanning electron microscope (ESEM), Fourier transform infrared spectroscopy (FT-IR), Raman spectroscopy and wide angle X-ray diffraction (WAXD) studies. Post-spinning treatment with methanol and/or stretching and co-electrospinning with single walled carbon nanotubes (CNT) were carried out to alter the strength, toughness, crystallinity and conductivity of silk nanofibers. Addition of just 1% CNT along with post-spinning treatments resulted in 7-fold increase in the strength and 35-fold increase in the modulus of silk nanofibers. Raman spectroscopy confirmed that CNTs were incorporated in the silk fibers. FT-IR spectroscopy and WAXD studies proved that silk–CNT nanofibers had more crystallinity compared to silk nanofibers without CNT. Four-probe method demonstrated that silk–CNT nanofibers had 4 times higher electrical conductivity compared to silk nanofibers without CNT.

© 2009 Elsevier Ltd. All rights reserved.

### 1. Introduction

Electrospinning is a unique method capable of producing nanoscale fibers from both synthetic as well as natural polymers for numerous applications [1–6]. Tissue engineering is one of the many applications for which nanofibers are employed [2]. The nanofibers produced from the regenerated *Bombyx mori* silk are the ideal candidates for generating scaffolds because of the superior mechanical properties of silk fibers and possibility of enhanced biocompatibility [7–10]. Regenerated silk protein is fabricated from degummed natural cocoon silk fibers by dissolving them in a concentrated salt solution, then dialyzed to remove salt and finally lyophilized to remove water. This regenerated silk can be converted to various forms including fibers, films, powders and filaments [3,11–13]. The regenerated silk is known to have lower mechanical properties than the natural cocoon fibers [3,14,15] mainly because of the structural changes happening in the process of regeneration. The silk produced by regeneration method has lower  $\beta$  sheet contents resulting in a lower crystallinity and hence

lower properties. An attempt was made to narrow the gap by altering the properties of silk nanofibers using post-spinning treatment and co-electrospinning method.

Methanol is known to induce crystallization in silk fibroin by forming  $\beta$  sheets [12,14,16–19]. It is well known in Textile fibers that physical annealing helps in the orientation of the crystals in the direction of pull. We hypothesize that post-spinning treatment of the silk nanofibers with methanol along with stretching will improve the mechanical properties of nanofibers. Another method for improving the properties is dispersing the particles in the fibers. Carbon nanotubes (CNTs) are one atom thick layers of graphite rolled into a cylinder. They are 1 nm in diameter and several microns in length. They are light weight, flexible and with elastic modulus of 1 TPa, tensile strength of 37 GPa and breaking elongation of 6–30% are the hitherto the toughest material known [20–22]. Since the discovery CNTs by Iijima they have become intensely studied material as the fillers for light weight and high strength composites [23,24]. Our previous studies have proved that addition of CNTs in spinning dope improves the mechanical properties [25,26] and it is possible to fabricate continuous uniform silk fibers of 100 nm in diameter varying electric field, spinning distance and concentration [27,28]. In this paper we present the post-spinning treatment with methanol and stretching and evaluation of structural, mechanical

\* Corresponding author. Tel.: +1 604 822 7945.

E-mail address: [frank.ko@ubc.ca](mailto:frank.ko@ubc.ca) (F. Ko).

and electrical properties of silk nanofiber nanocomposites for their potential use in tissue engineering scaffolds.

## 2. Materials and methods

### 2.1. Regenerated silk and spinning dope preparation

Silk fibers were obtained from Taiwan Textile Research Institute (TTRI). All reagents were purchased from Sigma Aldrich unless otherwise mentioned. The fibers were boiled in aqueous 0.02 M  $\text{Na}_2\text{CO}_3$  at 100 °C for 30 min and rinsed with water to extract sericin. These degummed fibers were dissolved in 50% aqueous  $\text{CaCl}_2$  at 100 °C, to obtain 6% silk solution. All concentration measurements were done in weight by weight (w/w). The solution was poured into regenerated cellulose dialysis tubing (Fisher Scientific: T3 membrane, pore size 25 Å) to carry out dialysis against 1 l of deionized water for 48 h at 23 °C. The regenerated silk fibroin sponge was obtained by lyophilization (Labconco 2.5 FreezonePlus lyophilizer). The spinning dope was prepared by dissolving regenerated silk sponge in formic acid.

### 2.2. Nanofibers and nanocomposite fabrication

The silk–formic acid spinning dope was transferred to 3 ml syringe with 18-G needle and electrospun at a 45° spinning angle with spinning conditions of 15% concentration, electric field of 3 kV/cm and distance of 10 cm. For obtaining aligned fibers a cardboard (secondary collection plate) was placed in between the syringe and the collection plate. The random fibers got deposited on the collection plate and aligned fibers were formed between a cardboard and the edge of the collection plate.

Nanocomposite scaffold fabrication was carried out by co-electrospinning regenerated silk in formic acid (w/w) along with single walled carbon nanotubes in the concentration 1% of silk. CNTs processed by high-pressure carbon monoxide (HiPCO) method were dispersed in the required amount of formic acid by sonication for 2 h. The necessary regenerated silk was added to this mixture and again sonicated for one more hour. This mixture was then stirred for 1 h prior to spinning. Both aligned and random fibers were fabricated using the secondary collection plate technique described earlier.

### 2.3. Post-spinning treatments

The random nanofiber mat was treated with 90:10 methanol–water (vol/vol) for 10 min. The mat was then rinsed with deionized water and allowed to dry in a vacuum chamber overnight. The aligned fibers were rolled in to a yarn and treated with methanol in a similar way. For mechanical annealing, the random mat was physically stretched in between an aluminum frame held together by clips from the length of 5 cm to 5.5 cm. Further stretching was avoided as it resulted into breakage of the mat. The rolled aligned fiber yarns were also stretched in a similar way from the length of 5 cm to 5.5 cm. For evaluating the effect of methanol as well as stretching the mat and the aligned yarns were first treated with methanol–water 90:10 (vol/vol) and rinsed with deionized water. They were then mounted on an aluminum frame and stretched

while they were still wet. They were allowed to dry overnight in a vacuum chamber.

### 2.4. Scaffold characterization

The morphology of the palladium sputtered electrospun fibers was examined and their diameters were determined by Phillips XL-30 ESEM. The average fiber diameter and its distribution were determined based on 100 random measurements. The composition of silk fibers was characterized by Nicolet Magna-IR 560 FT-IR spectrometer. The structure and crystallinity of fibers were determined by Siemens D500 WAXD. Raman Spectra (Renishaw 1000) were obtained using a 780 nm diode laser. Mechanical properties of both random and aligned nanofibers were determined by KES-G1 Kawabata micro-tensile tester at the elongation rate of 0.2 mm/s. For random mat, strips measuring 4 × 0.5 cm were glued on a paper frame and then mounted on Kawabata micro-tensile machine and average tensile properties from five samples were measured. The time in seconds required to break the sample was noted and converted to displacement (mm) by dividing it by elongation rate (0.2 mm/s). The displacement was converted to strain by dividing it by gauge length. The load on the strips was computed as gram force. The specific stress in g/Tex was then calculated using the following equation.

$$\text{Stress (g/Tex)} = \frac{\text{Force (g)}/\text{specimen width (mm)}}{\text{Areal density (g/m}^2\text{)}}$$

The areal density is simply the weight (g) of the nonwoven test strip divided by the area ( $\text{m}^2$ ) of the strip. The stress in g/Tex was converted to MPa using following equation.

$$\text{Stress (MPa)} = 9.8 \times \text{Stress (g/Tex)} \\ \times \text{density of material (g/cc)}$$

The aligned fibers were rolled into a yarn. The 4 cm long sample was glued from both the sides on a paper frame having 1 cm length. This gives us the gauge length of about 3 cm. These samples were then mounted on a Kawabata micro-tensile machine and the tensile properties were measured from the average of five samples. The weight and length of all the yarns were measured prior to mounting them on a paper frame. The linear density of the yarn expressed in the unit of denier (g/9000 m) was determined for each yarn. The load on the yarn was normalized by the linear density to obtain the specific stress expressed in gram force/denier. Knowing the density of the silk at 1.25 g/cc one can determine the engineering stress in MPa.

To measure the electrical conductivity we used Four-point probe method. The sample was mounted on a glass slide and the four probes of the machine were lowered on the sample. The length, width and the thickness of the sample were noted. The distance between the probes (probe space) was 2 cm. The known amount of current was passed through the sample and the voltage was read. The conductivity in Siemens/cm (S/cm) of the sample was measured using following equation.

### 2.5. Statistical analysis

The statistical significance was determined by the analysis of variance (ANOVA) and Tukey post-hoc test at the significance level

---


$$\text{Conductivity (S/cm)} = \frac{\text{Current (mA)} \times \text{length of the sample (cm)}}{\text{Voltage (mV)} \times \text{thickness of the sample (cm)} \times \text{probe space (cm)}}$$


---

of less than 0.05 ( $P < 0.05$ ) using SPSS 14 for Windows<sup>R</sup> software package.

### 3. Results

#### 3.1. Structure of silk nanofibers and silk–CNT nanocomposite

The protein conformation in natural cocoon silk fibers, electrospun nanofibers, methanol treated nanofibers and silk–CNT nanofibers were determined by FT-IR spectroscopy, Raman spectroscopy and WAXD.

The FT-IR spectra were collected using Nicolet Magna-IR 560 spectrometer and deconvoluted using Digilab Merlin 3.3 software (Fig. 1). The frequencies of amide regions in the natural cocoon fibers (Fig. 1A (1)) and nanofibers (Fig. 1A (2)) did not show any significant differences proving the protein composition remained unchanged. They were higher in the silk nanofibers treated with methanol (Fig. 1A (3)) and silk–CNT nanofibers (Fig. 1A (4)). FT-IR spectroscopy of silk fibroin shows 2 peaks in the Amide I region at 1650 and 1630. The ratios of areas under these peaks determine the configuration of the protein [29]. Amide I peak at 1630 represents  $\beta$  sheet configuration whereas at 1650 represents random coil and helical structure. The ratios of area under the curve for 1630 to total area under the curves for 1630 and 1650  $[\text{Area}_{1630}/(\text{Area}_{1650} + \text{Area}_{1630})] \times 100$  give you the percentage of  $\beta$  sheets in the sample. Our calculations proved that natural cocoon fibers had 65%, nanofibers had 62%  $\beta$  sheets, nanofibers after methanol treatment had 63.5% and nanofibers with 1% CNT had 64%  $\beta$  sheets.

The Raman spectroscopy is a very useful tool for determining the conformation of proteins in the solid as well as in solutions. It also helps us to determine chemical modification and crystallization. Raman spectra contain bands that are characteristic of the specific molecules in the sample (Fig. 2). There was no major difference in the frequency of the peaks in all samples (Fig. 2A). But the intensities were not same indicating a difference in alignment of the polypeptide backbone. Silk fibroin protein has characteristic bands in the range 1650–1667 and 1241–1279  $\text{cm}^{-1}$  corresponding

to Amide I and Amide III respectively [30]. We observed these bands at 1665  $\text{cm}^{-1}$  and 1231  $\text{cm}^{-1}$  in our samples (Fig. 2B). These regions showed a little higher intensity in the samples having methanol (Fig. 2B (3)) indicating better alignment of the polypeptide backbone after methanol treatment.

CNT shows very unique peaks in Raman spectroscopy. They have 3 characteristic peaks. The peak for Tangential Mode (TM) is observed between 1593 and 1570  $\text{cm}^{-1}$ . TM band can be used to differentiate metallic from semi-conducting nanotubes [31]. The Radial Breathing Mode (RBM) band arises between 195 and 270  $\text{cm}^{-1}$ . The RBM bands have a diameter-dependent frequency and can be used to determine the nanotubes' diameters [32]. The last characteristic peak is Disorder Induced Mode (D) and it is at 1299  $\text{cm}^{-1}$ . The D band provides the information on the crystallinity of the sample and the defects in the  $sp^2$  orbital of carbon in the nanotubes [33]. We carried out the Raman spectroscopy of CNT used in this study (Fig. 3). We were able to see all characteristic bands of CNT in our sample. The Raman spectra of silk nanofibers with and without CNT were taken as well. The similar characteristic peaks were observed in CNT reinforced silk nanofibers proving that CNT got incorporated in silk fibers during electrospinning.

The WAXD is a powerful technique for determining the three dimensional structure of molecules that form crystals or regular fibers. It can be used to determine the type, structure of the crystals and degree of orientation of the crystallites. We carried out WAXD on cocoon and nanofibers using copper radiation at 40 kV and 20 mA with collection of spectrum at  $\theta = 5$ –50 and step size of 0.1. The resemblance between diffraction patterns of cocoon and nanofibers suggests structural similarity between them (Fig. 4). The fibers had five diffraction peaks at 13.7, 16.5, 18.2, 25.3 and 28.1°, corresponding to d-spacings of 6.5, 5.4, 4.9, 3.5 and 3.2 Å respectively with higher intensities in methanol treated and CNT reinforced fibers. Bragg's law was used to calculate d-spacings. According to Bragg's law, d-spacing (d) which is an intercrystallite space is given by

$$d = \lambda/2(1/\sin \theta)$$

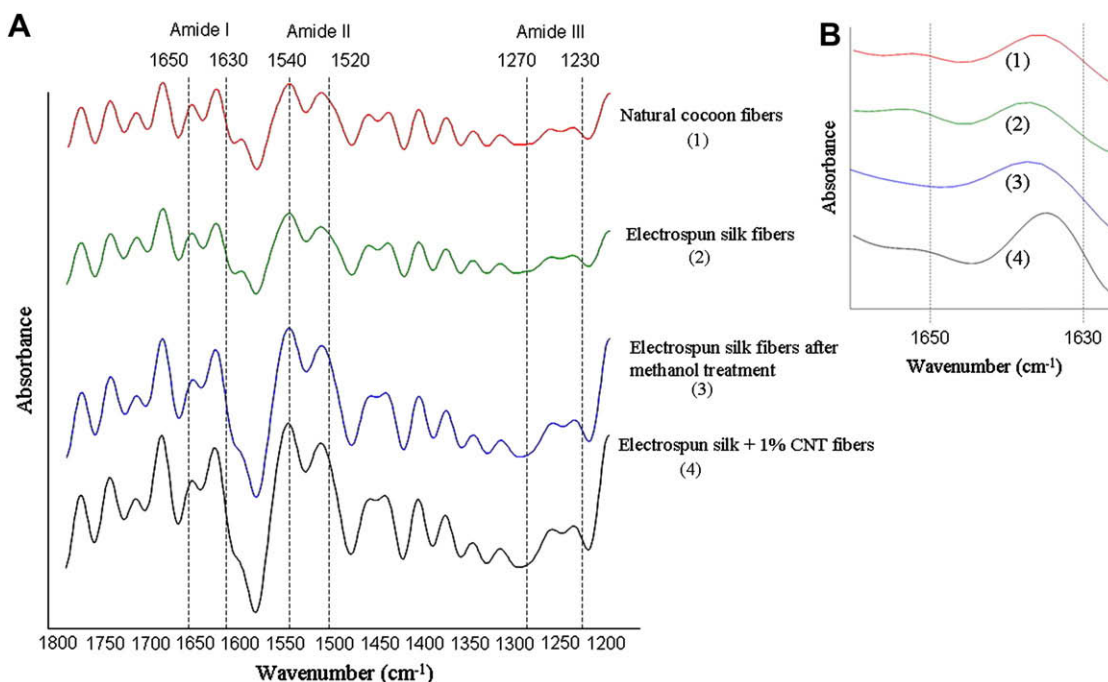


Fig. 1. FT-IR spectra (A) and amide I regions (B) of various silkworm silk fibers.

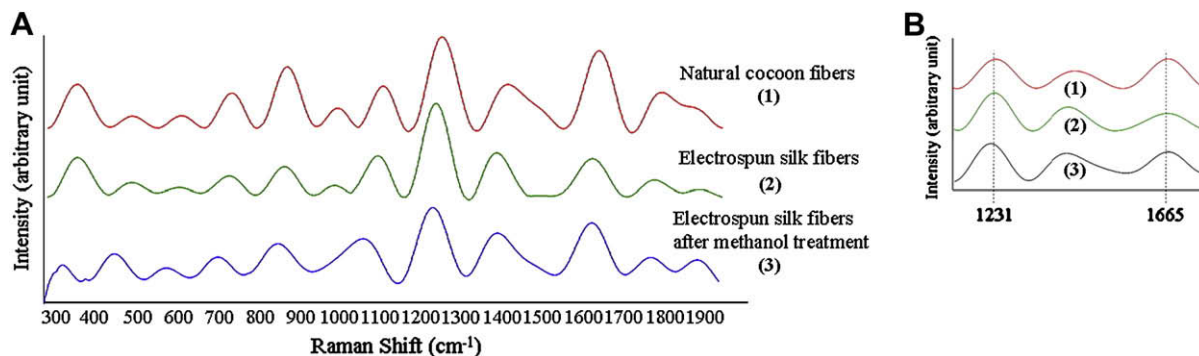


Fig. 2. Raman spectra (A) and Amide I and III (B) regions of various silkworm silk fibers.

where  $\lambda$  is the wavelength of copper (1.5406) and  $\theta$  is an incident angle. The natural silk protein exists in 2 forms, silk I and silk II. Silk I is the helical protein present in the silk glands prior to spinning. It is water soluble and undergoes a structural change to water insoluble silk II protein which is a fiber in  $\beta$  sheet form. The transition from silk I to silk II is known to occur because of many factors including acidic pH, removal of calcium ions and water molecules from the ducts along with the presence of external forces [34–36] during natural spinning process. In the present study, calculated d-spacings correspond to both silk I (3.5 and 3.2 Å) and silk II (5.4 and 4.9 Å) structure. The unknown d-spacing of 6.5 may be due to other types of conformations such as  $\beta$ -turns. Thus the fibers were predominantly made up of the crystals of  $\beta$  sheets dispersed in an amorphous matrix.

### 3.2. Effect of post-spinning treatments on diameter and mechanical properties

We tried to alter the tensile properties of silk nanofibers by post-spinning treatments of aligned as well as random fibers with methanol and stretching. The morphology of the palladium coated fibers was observed and their diameters determined before and after the treatment with methanol and stretching (Fig. 5).

Methanol treatment of the silk nanofibers leads to the contraction of the fibers thus increasing their average diameter. This was observed for both aligned as well as random fibers. The random mat had the average diameter of  $72 \pm 25$  nm and after methanol treatment the diameter was  $231 \pm 70$  nm. For the aligned fiber the diameter change observed was from  $90 \pm 60$  nm to  $233 \pm 60$  nm. Also, the methanol treated fibers were not as smooth in appearance as non-treated. They had a grainier or rougher surface. When the fibers were stretched along with the methanol immersion the fiber diameter did not change much. The average diameter of the random fibers after methanol and stretching was  $88 \pm 32$  nm, whereas that of aligned fibers was  $70 \pm 51$  nm (Table 1).

These six samples, random mat, random mat with methanol, random mat with methanol and stretching, aligned fibers, aligned fibers with methanol and aligned fibers with methanol and stretching were evaluated for the mechanical properties. The tensile properties of all these fibers were measured from 5 samples and the average stress–strain curves were plotted. The random mat had a modulus of  $140.67 \pm 2.21$  MPa, strength of  $6.18 \pm 0.3$  MPa and elasticity of  $5.78 \pm 0.65\%$  (Table 2). The aligned fibers had a modulus of  $174.98 \pm 2.86$  MPa, strength of  $7.75 \pm 0.4$  MPa and elasticity of  $5.05 \pm 0.45\%$  (Table 3). The treatment with methanol

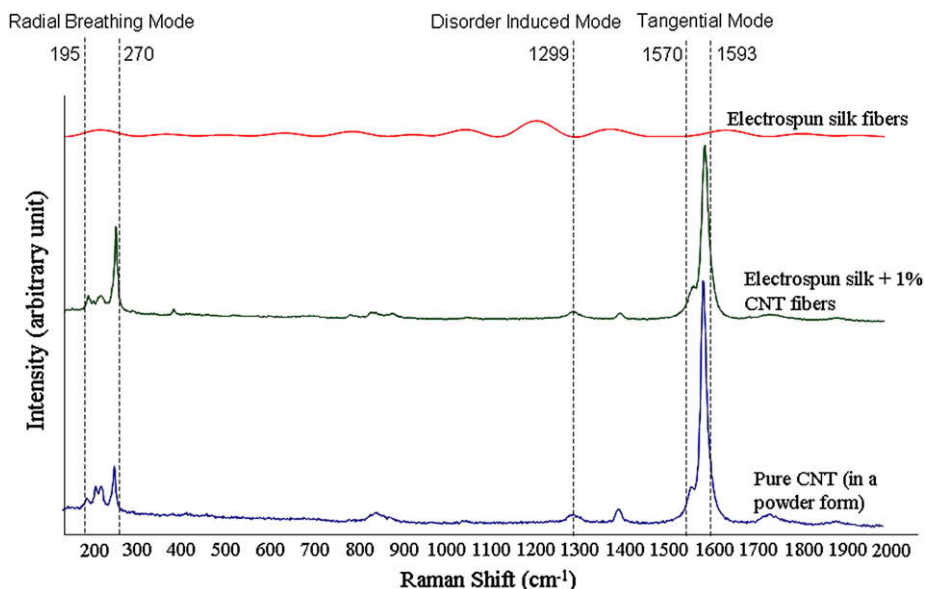


Fig. 3. Raman spectra of silkworm silk nanofibers with and without CNT. The pure CNT spectrum has the characteristic peaks which are observed in the CNT reinforced silk fibers as well.

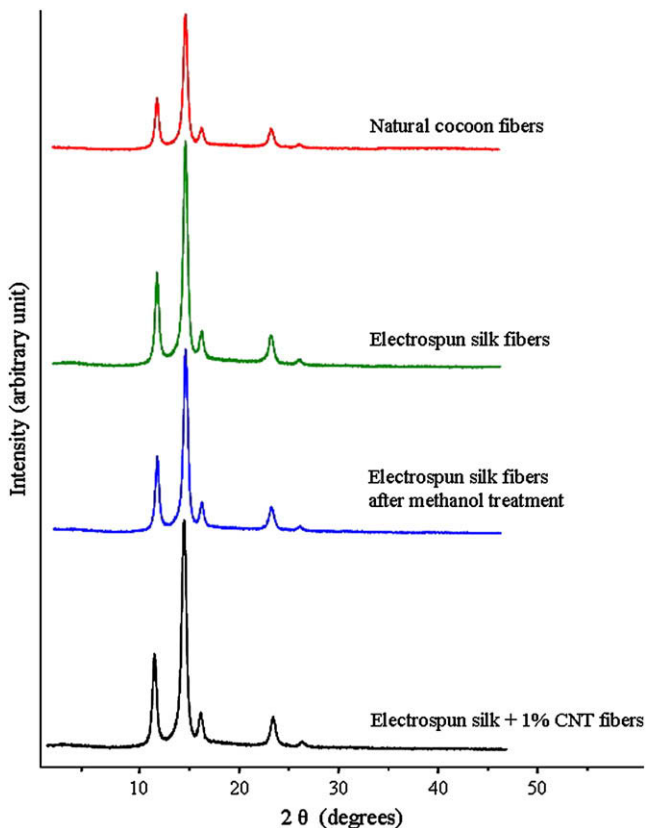


Fig. 4. WAXD of various silkworm silk fibers.

**Table 1**

Fiber diameter of the silk fibers with and without CNT.

Fiber	As-spun	Methanol	Methanol + stretching
Random	72 ± 25	231 ± 70	88 ± 32
Aligned	90 ± 60	233 ± 60	70 ± 51
Random + 1% CNT	153 ± 99	280 ± 92	140 ± 86
Aligned + 1% CNT	147 ± 41	288 ± 83	136 ± 53

to further improve the alignment of  $\beta$  sheets. Random mat after methanol treatment had a modulus of  $506.55 \pm 10.23$  MPa, strength of  $18.53 \pm 1.21$  MPa and elasticity of  $4.82 \pm 0.38\%$ . The aligned fibers after methanol treatment had a modulus of  $630.11 \pm 12.21$  MPa, strength of  $23.25 \pm 1.32$  MPa and elasticity of  $4.22 \pm 0.21\%$ . Stretching of the fibers along with methanol treatment further increased the properties. Random mat after methanol treatment and stretching had a modulus of  $729.89 \pm 15.43$  MPa, strength of  $22.23 \pm 0.98$  MPa and elasticity of  $4.01 \pm 0.22\%$ . The aligned fibers after methanol treatment and stretching had a modulus of  $995.015 \pm 15.76$  MPa, strength of  $26.38 \pm 1.97$  MPa and elasticity of  $2.78 \pm 0.14\%$ .

### 3.3. Effect of carbon nanotubes on mechanical properties and electrical conductivity

The silk nanofibers were reinforced with 1% CNT (w/w). The incorporation of CNT can alter the mechanical properties and can provide electrical conductivity to the scaffolds. The nanomat and aligned fibers produced by co-electrospinning silk and CNT were treated with methanol and stretching to calculate the tensile properties. Random nanofibers with CNT had the average diameter of  $153 \pm 99$  nm whereas that of the aligned fibers with CNT was  $147 \pm 41$ . The methanol treatment and stretching changed the fiber diameter of CNT reinforced fibers in a similar way as that of non-reinforced fibers (Table 1).

The incorporation of only 1% CNT significantly increased the tensile properties of both the random nanomat as well as the aligned fibers. These properties were further enhanced by methanol and stretching. Our calculations suggested that nanofiber mat with 1% CNT had modulus of  $633.84 \pm 12.94$  MPa, strength of  $13.89 \pm 0.9$  MPa and elasticity of  $2.89 \pm 0.17\%$ . The methanol treatment changed these properties to modulus of  $3644.25 \pm 30.34$  MPa, strength of  $44.46 \pm 2.34$  MPa and elasticity of  $1.61 \pm 0.43\%$ . The stretching accompanied by methanol treatment altered the properties to modulus of  $4817.24 \pm 69.23$  MPa, strength of  $44.46 \pm 2.1$  MPa and elasticity of  $1.22 \pm 0.14\%$  (Table 2). The aligned nanofiber showed the

significantly increased the tensile properties of the fibers. Methanol is known to induce crystals of  $\beta$  sheets in silk in various forms including nanofibers [17,18], conjugated films [14], and wet-spun fibers [12,16]. We believe methanol increases the mechanical properties by formation of  $\beta$  sheets. Mechanical properties of electrospun silk–polyethylene oxide nanofibers were evaluated by Wang et al. [37]. They utilized methanol–water treatment to remove polyethylene oxide from the composite nanofibers to yield pure silk nanofibers and to induce  $\beta$  sheets formation. The WAXD and FT-IR spectroscopic studies showed the conversion of silk from coil to  $\beta$  sheets and the peaks were indicative of the random orientation of fibers. In the present study, we employed post-spinning methanol treatment along with stretching as an attempt

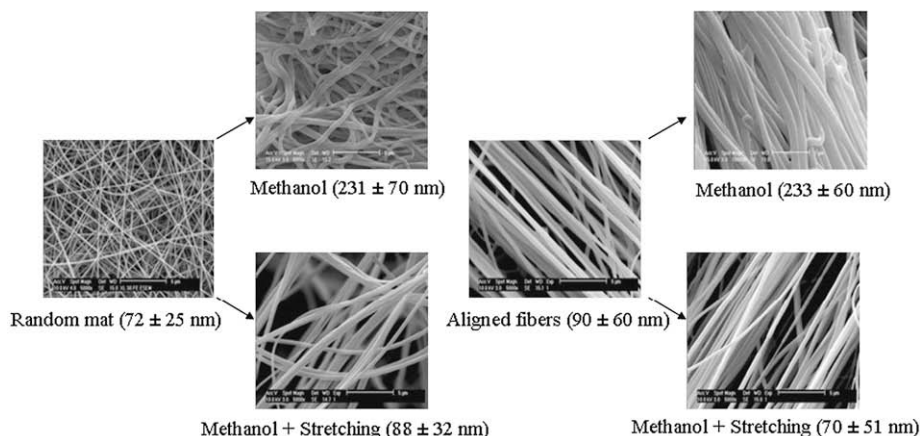


Fig. 5. Morphology and diameters of silkworm silk aligned and random nanofibers before and after methanol treatment and stretching.



**Table 2**  
Comparison of the mechanical properties of various silkworm silk nanofiber mats.

	Modulus (MPa)	Strength (MPa)	Elongation (%)
Nanomat	140.67 ± 2.21	6.18 ± 0.3	5.78 ± 0.65
Nanomat + methanol	506.55 ± 10.23	18.53 ± 1.21	4.82 ± 0.38
Nanomat + methanol + stretching	729.89 ± 15.43	22.23 ± 0.98	4.01 ± 0.22
Nanomat + 1% CNT	633.84 ± 12.94	13.89 ± 0.9	2.89 ± 0.17
Nanomat + 1% CNT + methanol	3644.25 ± 30.34	44.46 ± 2.34	1.61 ± 0.43
Nanomat + 1% CNT + methanol + stretching	4817.24 ± 69.23	44.46 ± 2.1	1.22 ± 0.14

similar trend. The aligned nanofibers with 1% CNT had the modulus, strength and elasticity of  $1269.37 \pm 20.58$  MPa,  $25.57 \pm 1.38$  MPa and  $2.3 \pm 0.34\%$  respectively. The methanol treatment of aligned fibers reinforced with CNT changed the modulus, strength and elasticity to  $4640.9 \pm 78.34$  MPa,  $53.47 \pm 2.87$  MPa and  $1.32 \pm 0.08\%$  respectively (Table 3). When the methanol treatment was accompanied with stretching they had modulus, strength and elasticity of  $6549.30 \pm 95.8$  MPa,  $58.04 \pm 2.86$  MPa and  $0.93 \pm 0.09\%$  respectively.

Electrical conductivity of silk nanofiber mats with and without CNTs was measured using four-point probe method. The conductivity of silkworm cocoon fibers was evaluated as well as a control. The samples were considered as films for the simplicity of calculation. The cocoon fibers had the conductivity of 0.016 S/cm whereas that of nanofibers and nanofibers with CNTs was 0.028 and 0.114 S/cm respectively. The cocoon fibers are the least conductive material. The nanofibers have higher conductivity. The addition of only 1% CNT significantly increases the conductivity of nanofibers.

#### 4. Discussion

An attempt was made in this paper to alter the properties of electrospun regenerated silk nanofibers by post-spinning treatments. These properties are an order of magnitude less than the natural cocoon fibers. However, the data presented in this study showed the improvement in the properties over the published information. Gotoh et al. [14] fabricated films from regenerated silk protein. They used lithium bromide as a salt solution and after dialysis they casted the films in the bath containing methanol. Their data suggested the strength of 16.37 MPa and elongation of 1.9%. Jin et al. produced silk nanofibers from regenerated silk protein [3,15]. They used lithium bromide as a salt solution and then added PEO in various concentrations to a dialyzed silk solution to make a spinable dope for electrospinning. After generating a nanofibrous structure from silk-PEO solution they removed PEO to obtain

**Table 3**  
Comparison of the mechanical properties of various aligned silkworm silk nanofibers.

	Modulus (MPa)	Strength (MPa)	Elongation (%)
Aligned nanofibers	174.98 ± 2.86	7.75 ± 0.4	5.05 ± 0.45
Aligned nanofibers + methanol	630.11 ± 12.21	23.25 ± 1.32	4.22 ± 0.21
Aligned nanofibers + methanol + stretching	995.015 ± 15.76	26.38 ± 1.97	2.78 ± 0.14
Aligned nanofibers + 1% CNT	1269.37 ± 20.58	25.57 ± 1.38	2.3 ± 0.34
Aligned nanofibers + 1% CNT + methanol	4640.9 ± 78.34	53.47 ± 2.87	1.32 ± 0.08
Aligned nanofibers + 1% CNT + methanol + stretching	6549.30 ± 95.8	58.04 ± 2.86	0.93 ± 0.09

a structure containing only silk nanofibers. The tensile properties of PEO extracted silk fibers after methanol treatment was 2 MPa of strength and 1.4% elongation. Additionally, we used co-electrospinning technique to generate silk-CNT nanofibers and to improve mechanical as well as electrical properties. The rationale for using CNT was elongation balance theory [38,39] according to which combining materials with similar elongation at break provide the most effective means of transferring tensile properties. On the basis of this theory, silk (15–20% elongation at break) and CNT (6–30% elongation at break) are the most compatible material systems. It has been demonstrated by Ko et al. that co-electrospinning provides an excellent method for aligning CNT in polymer fibril matrix [24]. Mechanical properties of nanocomposites prepared by them using co-electrospinning 1–5% CNT (w/w) in a polyacrylonitrile nanofiber matrix suggested a 4- to 5-fold increase in the properties [40]. We theorize that the improvement in the tensile properties after methanol and stretching is due to formation and orientation of  $\beta$  sheet crystals in nanofibers. Also, authors believe that CNT possibly is acting as a nucleating site for the growth of these crystals. However, further analysis using appropriate technology similar to 2D WAXD, NMR, TEM and/or polarized spectroscopy is necessary in order to substantiate these claims.

#### 5. Conclusions

The regenerated silk was successfully electrospun in formic acid to generate nanofibers. The silk nanofibers were reinforced with 1% CNT to improve mechanical and electrical properties. The process optimization and characterization were carried out on various nanofiber nanocomposites. Uniform fibers with diameter less than 100 nm were produced in the spinning conditions of concentration range 12–15% (w/w) and electric field of 3–4 kV/cm. Secondary collection plate technique was found to be an effective way of fabricating aligned nanofibers. Post-spinning treatment with methanol and stretching increased the mechanical properties significantly. These treatments improved the crystallinity of fibers as well which was investigated by FT-IR and WAXD studies. Methanol induces the formation of  $\beta$  sheets in nanofibers. Stretching helps in aligning the fibers to the direction of pull. We were successfully able to incorporate CNT in nanofibers as evident from Raman spectroscopy. FT-IR spectroscopy and WAXD studies showed that silk-CNT nanofibers had more crystallinity compared to silk nanofibers without CNT. The strength and toughness of silk fibers were significantly increased upon addition of just 1% CNT. Electrical conductivity was improved as well with CNT. For tissue engineering of load bearing tissue which also requires electrical conductivity for cell growth, example bone [41], silk-CNT nanofiber nanocomposites should help scientists fabricate specific scaffolds for their applications.

#### Acknowledgements

This work was supported in part by Pennsylvania Nanotechnology Institute. Authors acknowledge the financial support from Taiwan Textile Research Institute. The NSF Grant number DMR-0116645 and BES-0216343 supported the purchase of Raman spectrometer and ESEM respectively.

#### References

- [1] Zong X, Li S, Chen E, Garlick B, Kim KS, Fang D, et al. *Annals of Surgery* 2004;240(5):910–5.
- [2] Doshi J, Reneker DH. *Journal of Electrostatics* 1995;35(2–3):151.
- [3] Jin HJ, Fridrikh SV, Rutledge GC, Kaplan DL. *Biomacromolecules* 2002; 3(6):1233–9.
- [4] Li WJ, Laurencin CT, Caterson EJ, Tuan RS, Ko FK. *Journal of Biomedical Materials Research* 2002;60(4):613–21.

- [5] Deitzel JM, Kleinmeyer J, Harris D, Beck Tan NC. *Polymer* 2001;42(1):261.
- [6] Formhals A. Process and apparatus for preparing artificial threads. U.S. patent 1,975,504. In: Office USPat, editor, vol. 1,975,504: Gastell, R.S.; 1934. p. 7.
- [7] Santin M, Motta A, Freddi G, Cannas M. *Journal of Biomedical Materials Research* 1999;46(3):382–9.
- [8] Meinel L, Hofmann S, Karageorgiou V, Kirker-Head C, McCool J, Gronowicz G, et al. *Biomaterials* 2005;26(2):147–55.
- [9] Huang JK, Li M. *Zhongguo Xiu Fu Chong Jian Wai Ke Za Zhi* 2004;18(2):127–30.
- [10] Altman GH, Diaz F, Jakuba C, Calabro T, Horan RL, Chen J, et al. *Biomaterials* 2003;24(3):401–16.
- [11] Jin HJ, Park J, Valluzzi R, Cebe P, Kaplan DL. *Biomacromolecules* 2004;5(3):711–7.
- [12] Um IC, Kweon H, Lee KG, Ihm DW, Lee JH, Park YH. *International Journal of Biological Macromolecules* 2004;34(1–2):89–105.
- [13] Um IC, Ki CS, Kweon H, Lee KG, Ihm DW, Park YH. *International Journal of Biological Macromolecules* 2004;34(1–2):107–19.
- [14] Gotoh Y, Tsukada M, Baba T, Minoura N. *Polymer* 1997;38(2):487–90.
- [15] Jin HJ, Chen J, Karageorgiou V, Altman GH, Kaplan DL. *Biomaterials* 2004;25(6):1039–47.
- [16] Trabbic KA, Yager P. *Macromolecules* 1998;31(2):462–71.
- [17] Jeong L, Lee KY, Liu JW, Park WH. *International Journal of Biological Macromolecules* 2006;38(2):140–4.
- [18] Kim SH, Nam YS, Lee TS, Park WH. *Polymer Journal* 2003;35(2):185–90.
- [19] Wilson D, Valluzzi R, Kaplan D. *Biophysical Journal* 2000;78(5):2690–701.
- [20] Lu JP. *Physical Review Letters* 1997;79(7):1297–300.
- [21] Meyyappan M. *Carbon nanotubes: science and applications*. Boca Raton: CRC Press; 2005.
- [22] Wong EW, Sheehan PE, Lieber CM. *Science* 1997;277(5334):1971–5.
- [23] Bhattacharyya AR, Sreekumar TV, Liu T, Kumar S, Ericson LM, Hauge RH, et al. *Polymer* 2003;44(8):2373.
- [24] Ko FK, Khan S, Ali A, Gogotsi Y, Naguib N, Yang G. Structure and properties of carbon nanotube reinforced nanocomposites 43rd American institute of aeronautics and astronautics: AIAA/ASME/ASCE/AHS/ASC structures, structural dynamics, and materials conference. Denver, Colorado; 2002.
- [25] Ayutsede J, Gandhi M, Sukigara S, Ye H, Hsu CM, Gogotsi Y, et al. *Biomacromolecules* 2006;7(1):208–14.
- [26] Ayutsede J, Gandhi M, Sukigara S, Micklus M, Chen H-E, Ko F. *Polymer* 2005;46(5):1625–34.
- [27] Sukigara S, Gandhi M, Ayutsede J, Micklus M, Ko F. *Polymer* 2004;45(11):3701–8.
- [28] Sukigara S, Gandhi M, Ayutsede J, Micklus M, Ko F. *Polymer* 2003;44(19):5721–7.
- [29] Miyazawa T, Blout ER. *Journal of the American Chemical Society* 1961;83:712–9.
- [30] Rousseau ME, Lefevre T, Beaulieu L, Asakura T, Pezolet M. *Biomacromolecules* 2004;5(6):2247–57.
- [31] Filho AGS, Jorio A, Samsonidze GG, Dresselhaus G, Saito R, Dresselhaus MS. *Nanotechnology* 2003;14(10):1130–9.
- [32] Dresselhaus MS, Dresselhaus G, Pimenta MA, Eklund PC. *Raman scattering in carbon materials*. In: Pelletier MJ, editor. *Analytical applications of Raman spectroscopy*. London: Blackwell Science; 1999. p. 367–426.
- [33] Tan P, Dimovski S, Gogotsi Y. *Philosophical Transactions. Series A, Mathematical, Physical, and Engineering Sciences* 1824;2004(362):2289–310.
- [34] Guiyang L, Ping Z, Zhengzhong S, Xun X, Xin C, Honghai W, et al. *European Journal of Biochemistry* 2001;268:6600–6.
- [35] Inoue S, Tanaka K, Arisaka F, Kimura S, Ohtomo K, Mizuno S. *The Journal of Biological Chemistry* 2000;275(51):40517–28.
- [36] Vollrath F, Knight DP. *Nature* 2001;410(6828):541–8.
- [37] Wang M, Jin H-J, Kaplan DL, Rutledge GC. *Macromolecules* 2004;37(18):6856–64.
- [38] Ko FK, Krauland K, Scardino F. Weft Insertion Warp Knit for hybrid composites, progress in science and engineering of composites. In: Hayashi T, Kawata K, Umekawa S, editors. *ICCM-4 Proceedings of the fourth international conference on composites*, vol. 2. Tokyo, Japan: Japan Society for Composite Materials; 1982. p. 1169–84.
- [39] Averston J, Cooper G, Kelly A. *Properties of fiber composites*. National physical laboratory, Guildford, UK: IPC Science and Technology Press Ltd.; November 4th, 1971. p. 15.
- [40] Ko FK, Gogotsi Y, Ali A, Naguib N, Ye H, Yang GL, et al. *Advanced Materials* 2003;15(14):1161–5.
- [41] Anderson JC, Eriksson C. *Nature* 1970;227(5257):491–2.